Supporting Materials

Solving an Old Puzzle: Elucidation and Evaluation of the Binding Mode of Salvinorin A at the Kappa Opioid Receptor

Kristina Puls and Gerhard Wolber*

Department of Biology, Chemistry and Pharmacy, Institute of Pharmacy, Freie Universität Berlin; Königin-Luise-Str. 2+4, 14195 Berlin, Germany

*Correspondence: gerhard.wolber@fu-berlin.de (G.W.), Tel.: +49-30-838-52686

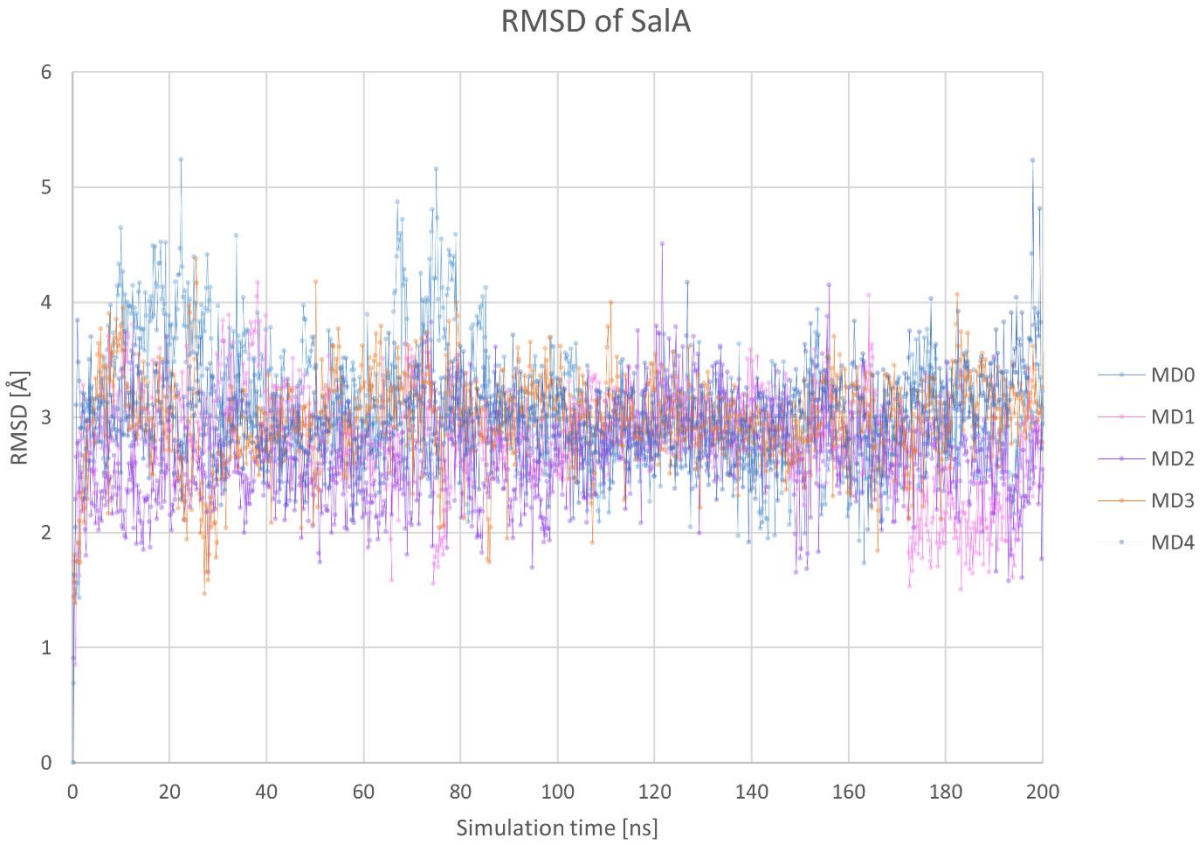

Figure S1. Root mean square deviation of SalA (**1**) in complex with the kappa opioid receptor (KOR) over the simulation time.

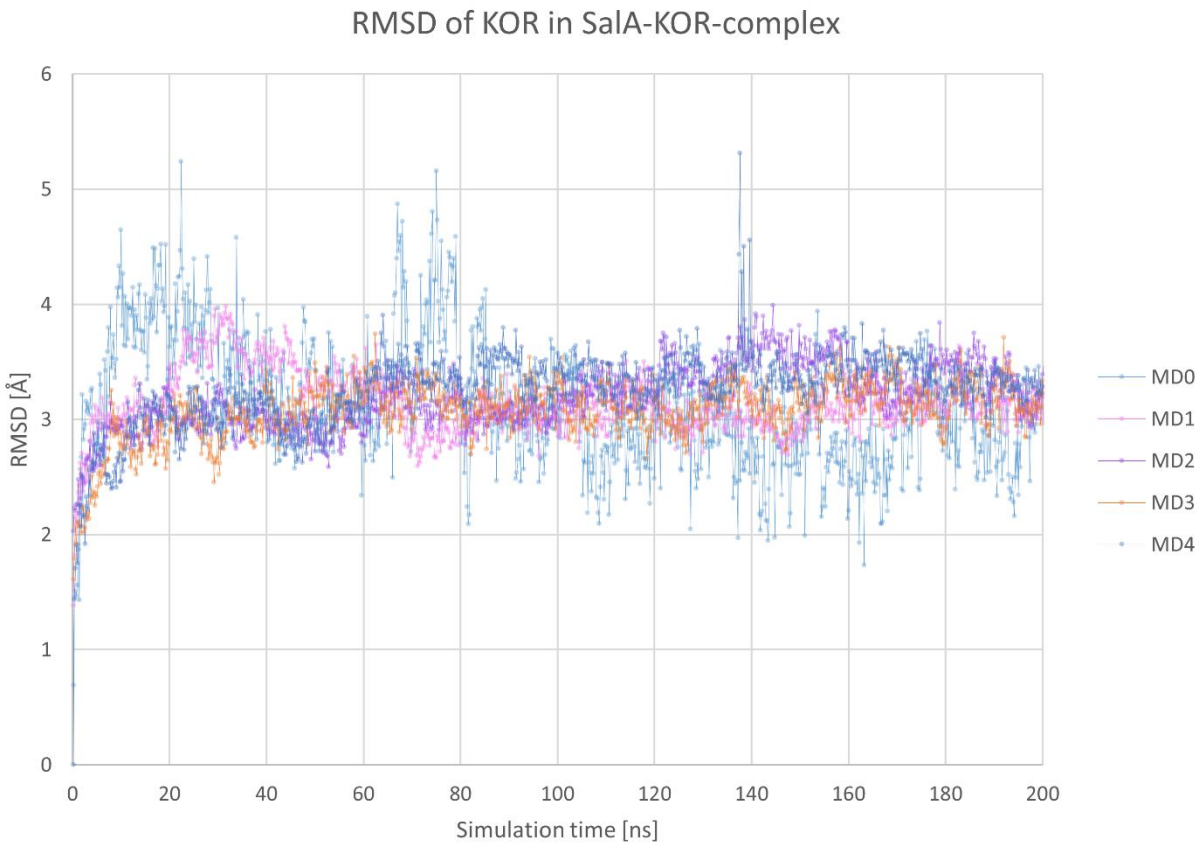

Figure S2. Root mean square deviation of the KOR backbone atoms in complex with SalA (**1**) over the simulation time.

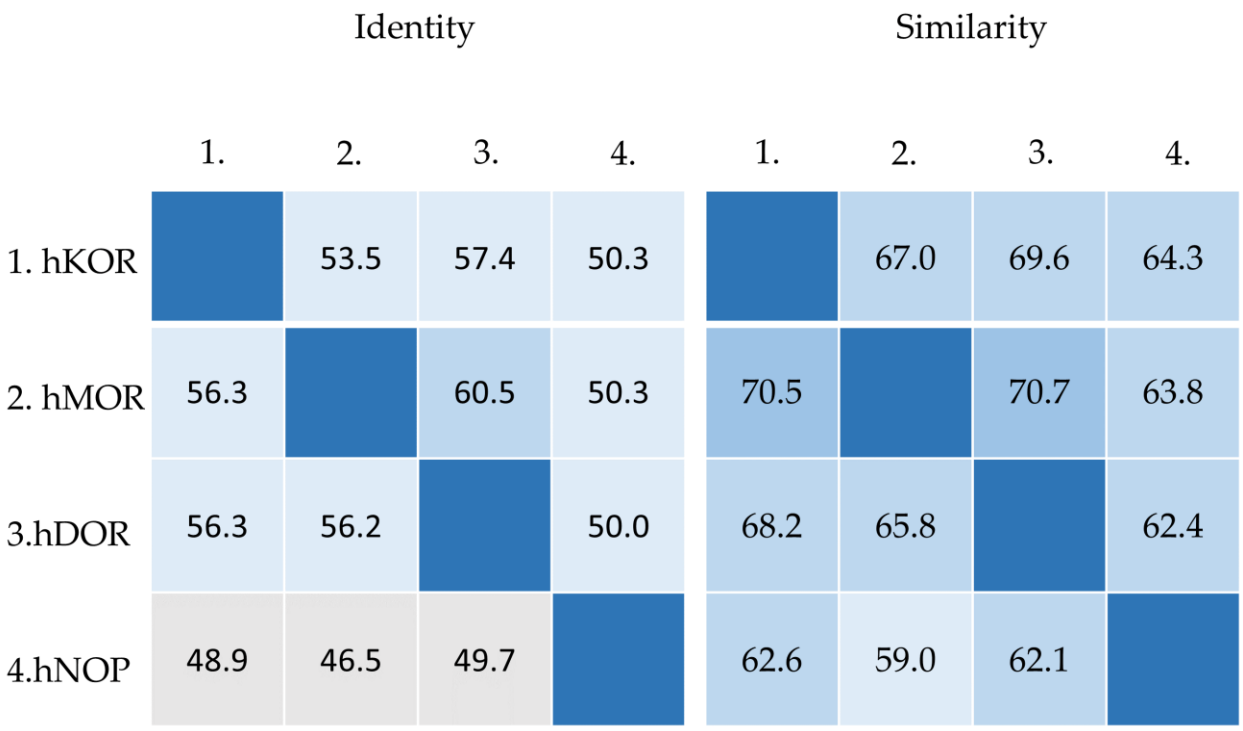

Figure S3. Sequence identity and similarity of the full sequence of KOR, MOR, DOR, and NOP.

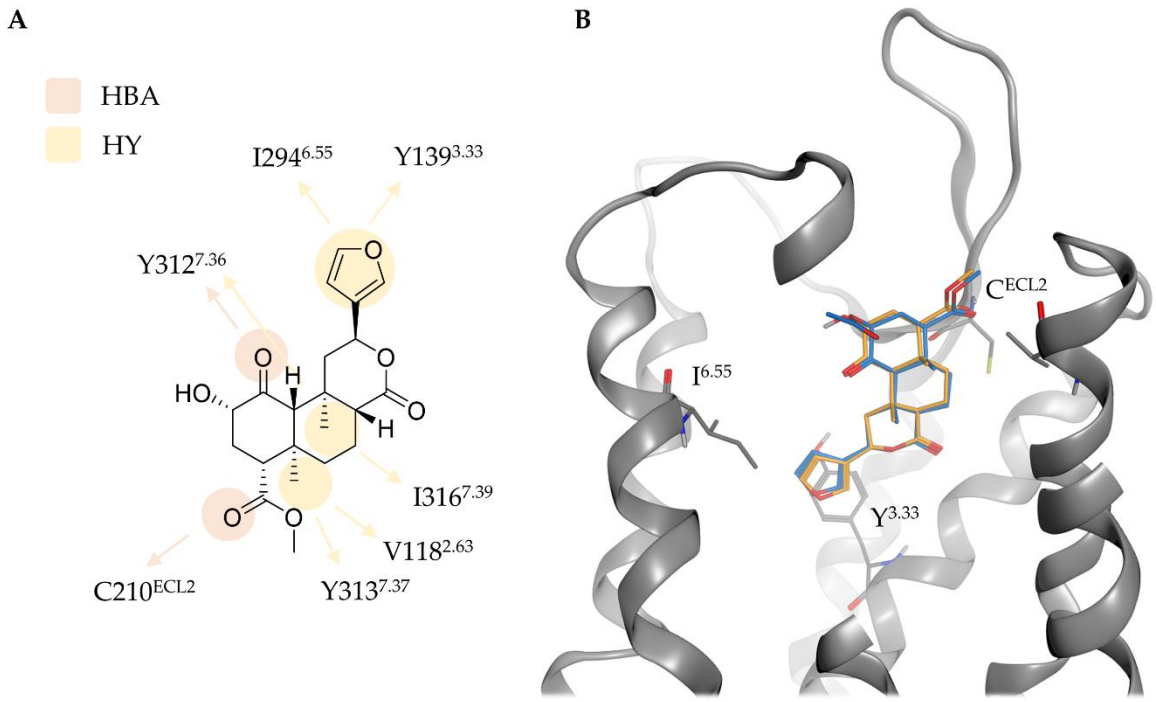

Figure S4. Protein-ligand interactions (A) and binding mode (B) of **2** (orange) at the KOR in comparison to SalA (blue). $Y^{3.33}$ denotes to $Y139^{3.33}$, C^{ECL2} to $C210^{ECL2}$, and $I^{6.55}$ to $I294^{6.55}$. Interactions types are abbreviated with HBA for hydrogen bond acceptor and HY for hydrophobic contact.

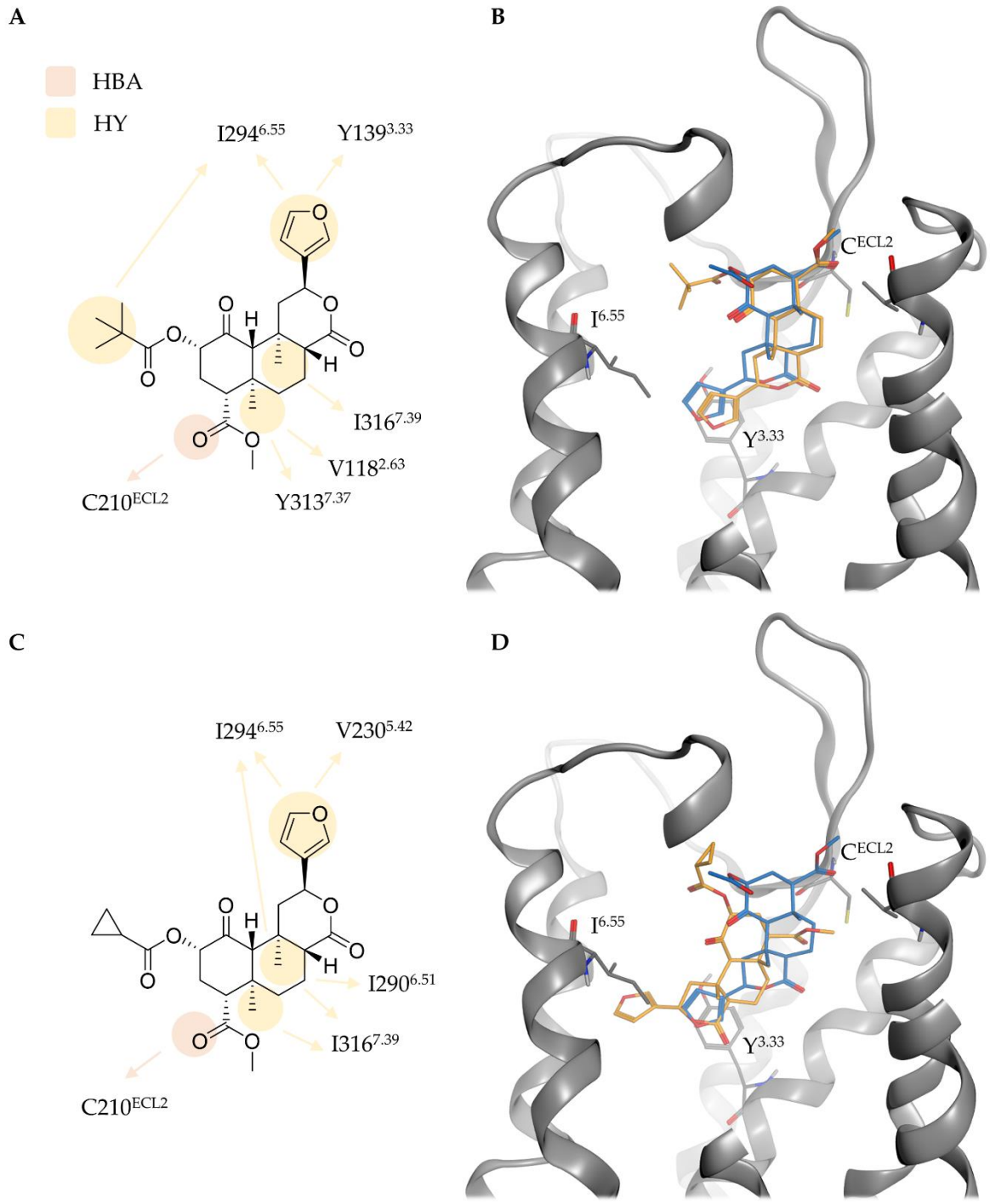

Figure S5. Protein-ligand interactions and binding mode of **3** (A, B, orange) and **4** (C, D, orange) at the KOR in comparison to SalA (blue). $Y^{3.33}$ denotes to $Y139^{3.33}$, C^{ECL2} to $C210^{ECL2}$, and $I^{6.55}$ to $I294^{6.55}$. Interactions types are abbreviated with HBA for hydrogen bond acceptor and HY for hydrophobic contact.

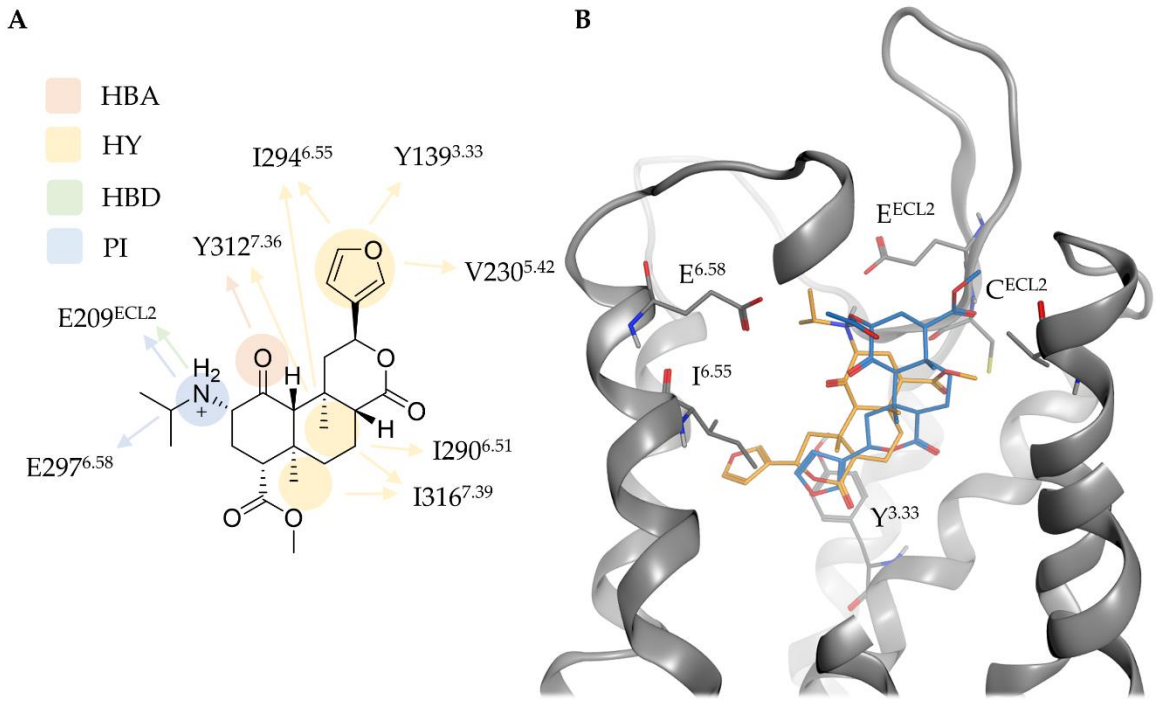

Figure S6. Protein-ligand interactions (A) and binding mode (B) of **5** (orange) at the KOR in comparison to SalA (blue). $Y^{3.33}$ denotes to $Y139^{3.33}$, C^{ECL2} to $C210^{ECL2}$, and $I^{6.55}$ to $I294^{6.55}$. Interactions types are abbreviated with HBA for hydrogen bond acceptor, HY for hydrophobic contact, HBD for hydrogen bond donor, and PI for positive charged interaction.

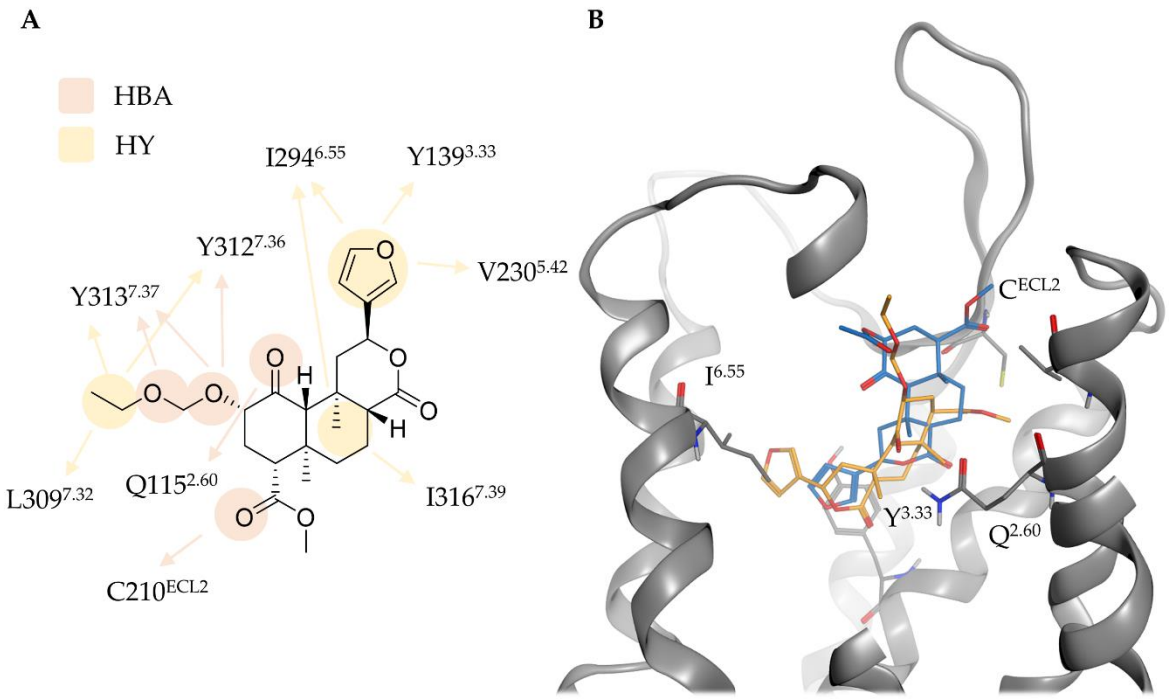

Figure S7. Protein-ligand interactions (A) and binding mode (B) of **6** (orange) at the KOR in comparison to SalA (blue). $Y^{3.33}$ denotes to $Y139^{3.33}$, C^{ECL2} to $C210^{ECL2}$, and $I^{6.55}$ to $I294^{6.55}$. Interactions types are abbreviated with HBA for hydrogen bond acceptor and HY for hydrophobic contact.

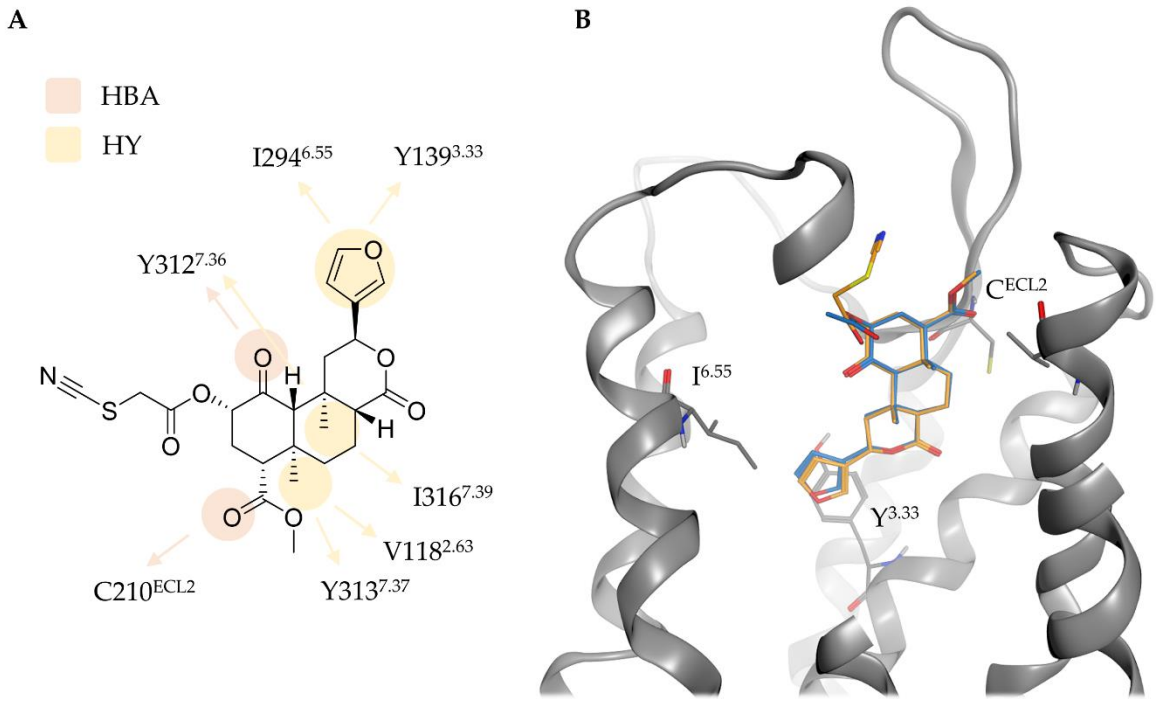

Figure S8. Protein-ligand interactions (A) and binding mode (B) of **7** (orange) at the KOR in comparison to SalA (blue). $Y^{3.33}$ denotes to $Y139^{3.33}$, C^{ECL2} to $C210^{ECL2}$, and $I^{6.55}$ to $I294^{6.55}$. Interactions types are abbreviated with HBA for hydrogen bond acceptor and HY for hydrophobic contact.

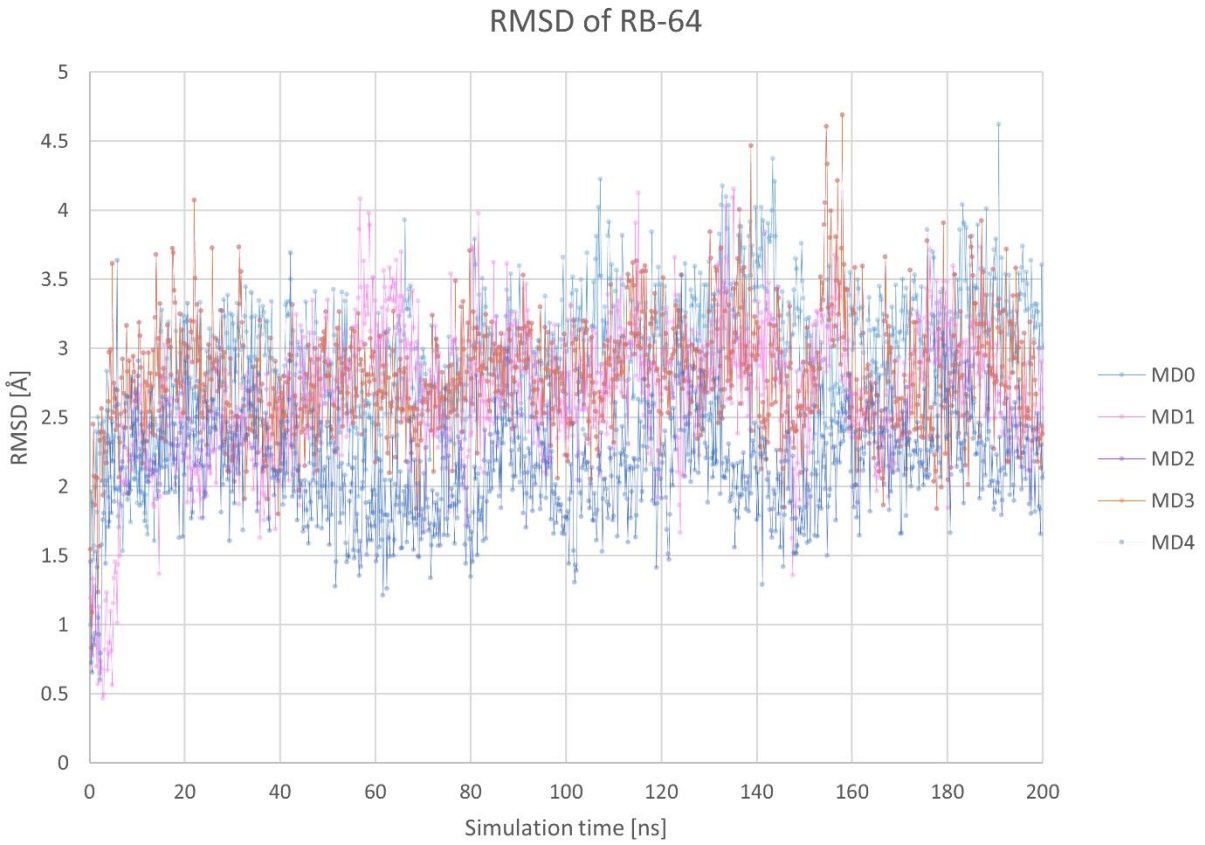

Figure S9. Root mean square deviation of RB-64 (**7**) in complex with the KOR over the simulation time.

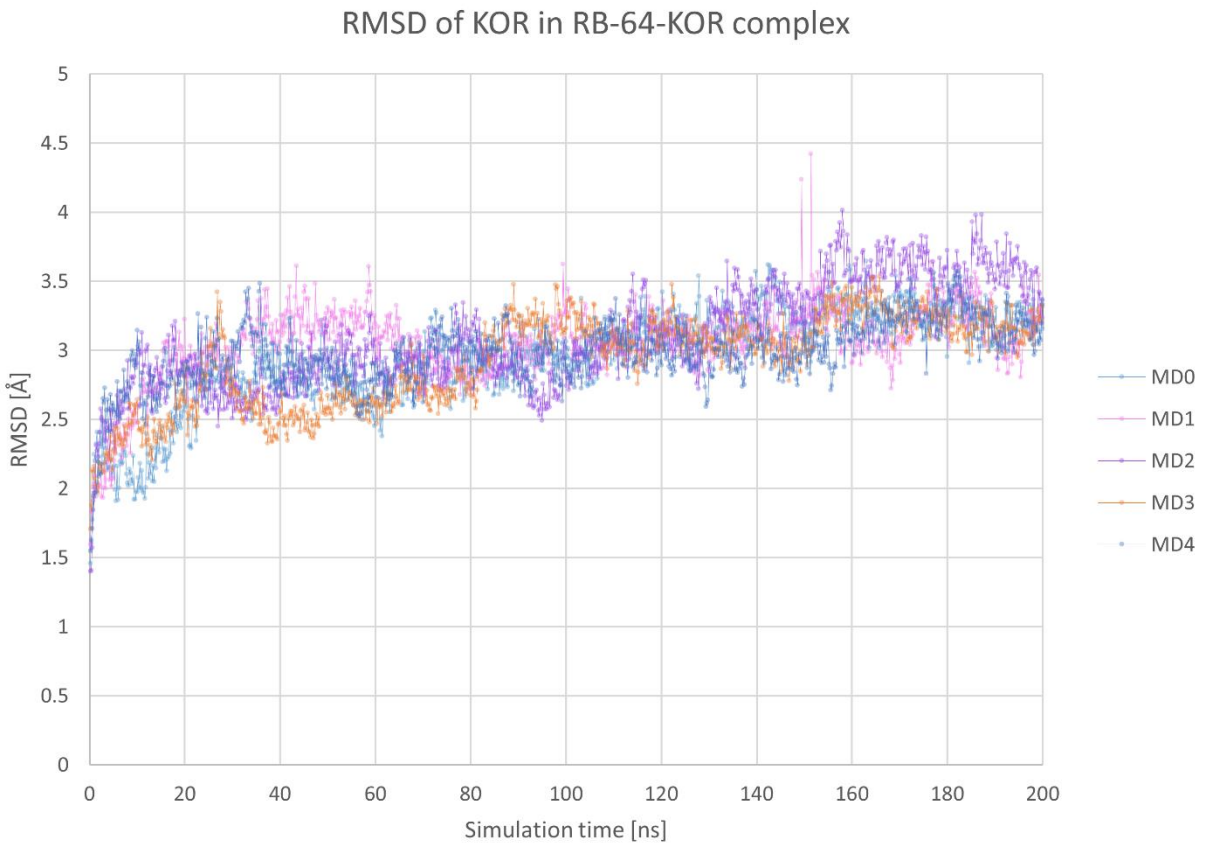

Figure S10. Root mean square deviation of the KOR backbone atoms in complex with RB-64 (**7**) over the simulation time.

Table S1. Energy calculations performed for the docking poses of SalA and RB64 bounded to the KOR.

RBFE				
Software	**Calculation**	**ΔG complex (kcal/mol)**	**ΔG solvent (kcal/mol)**	**RBFE (kcal/mol)**
Openfe [1]	Alchemical transformation of SalA into RB-64 bound to KOR	-27.273 ± 0.379	-25.059 ± 0.016	-2.214 ± 0.395
Schrödinger Ligand FEP [2,3]	Free energy perturbation turning RB-64 to SalA bound to KOR, respectively	-2.020 ± 0.202	-2.519 ± 0.214	0.499 ± 0.416
ABFE				
Software	**Calculation**	**ABFE (kcal/mol)**	**Difference in ABFE (kcal/mol)**	
YANK [4]	Binding free energy of SalA bound to KOR	-16.637 ± 0.961	|ABFE(SalA)| – |ABFE(RB-64)| = -3.817 ± 2.03	
	Binding free energy of RB-64 bound to KOR	-20.454 ± 1.069		

The abbreviations RBFE and ABFE refer to relative and absolute binding free energy. All methods predicted the binding of RB-64 to the active state KOR crystal structure (PDB-ID 6B73 [5]) favorable over the binding of SalA. The negative RBFE value in the case of openfe, where SalA is alchemically transformed into Rb-64, indicates that the latter (Rb-64) is favored over the first (SalA). The positive RBFE value in the case of Schrödinger Ligand FEP, where RB-64 is transformed into SalA, indicates the favorable binding of the first (RB-64) over the latter (SalA). In the case of YANK the absolute binding free energy of the two complexes, SalA or RB-64 bound to KOR, was calculated and compared. The more negative value for the RB-64 bound complex indicates an energetic improvement of the RB-64 bound state over the SalA-bound state.

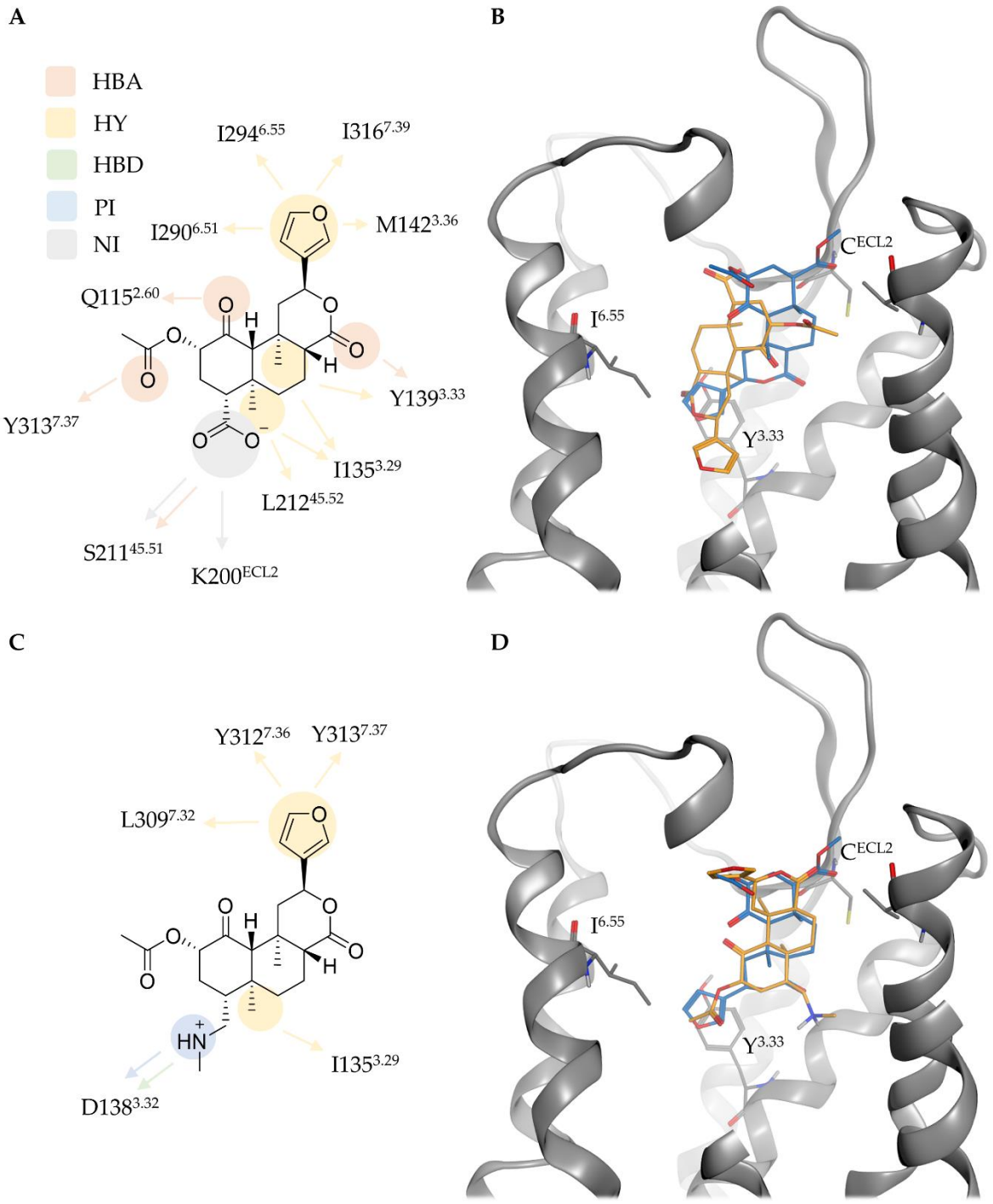

Figure S11. Protein-ligand interactions and binding mode of **8** (A, B, orange) and **9** (C, D, orange) at the KOR in comparison to SalA (blue). **8** is shifted in the binding side and shows an alternative Y139$^{3.33}$, C^{ECL2} to C210^{ECL2}, and I$^{6.55}$ to I294$^{6.55}$. Interactions types are abbreviated with HBA for hydrogen scaffold orientation while **9** shows a reversed orientation compared to SalA. Y$^{3.33}$ denotes to bond acceptor, HY for hydrophobic contact, HBD for hydrogen bond donor, NI for negative charged interaction, and PI for positive charged interaction.

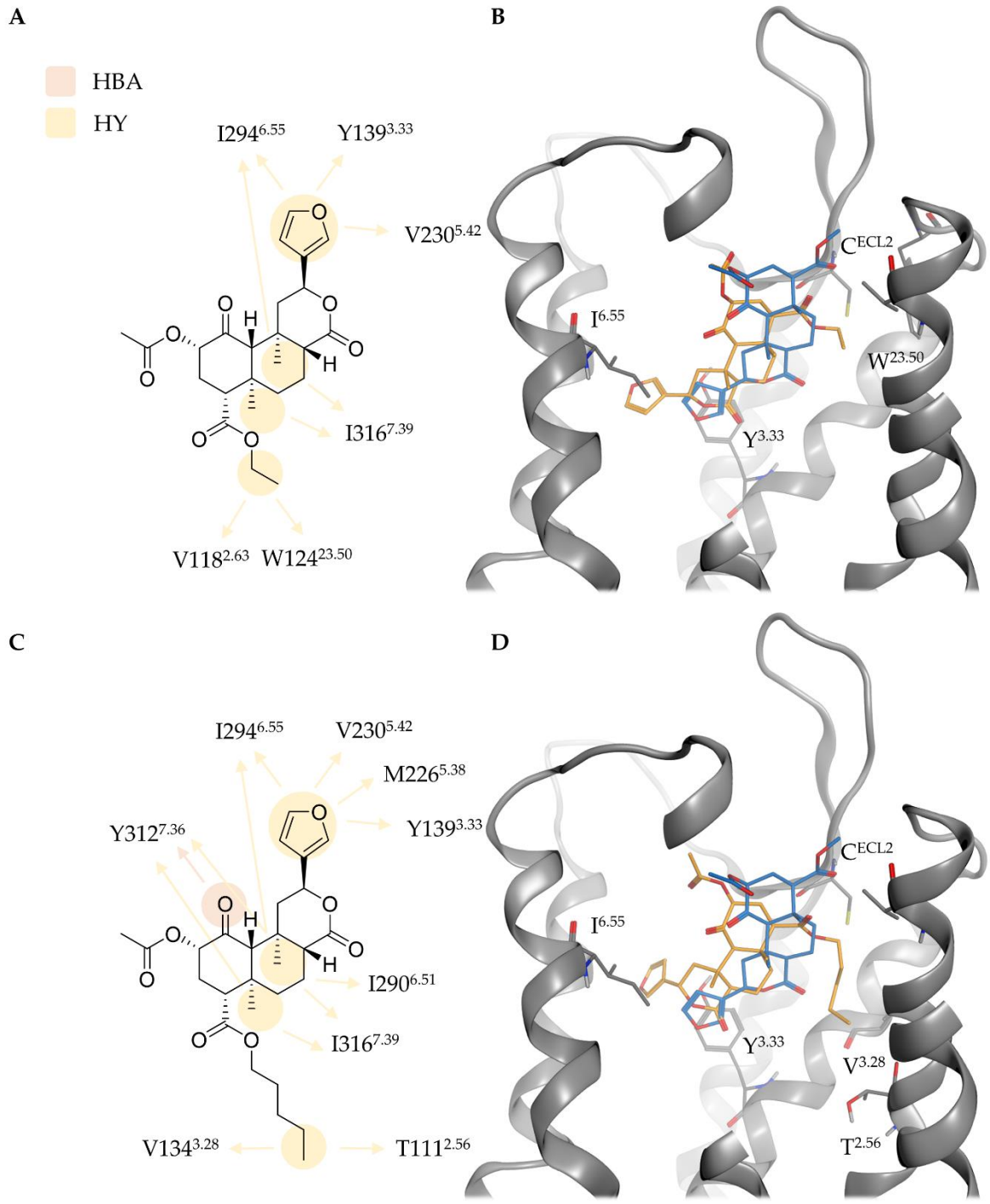

Figure S12. Protein-ligand interactions and binding mode of **10** (A, B, orange) and **11** (C, D, orange) at the KOR in comparison to SalA (blue). $Y^{3.33}$ denotes to $Y139^{3.33}$, C^{ECL2} to $C210^{ECL2}$, and $I^{6.55}$ to $I294^{6.55}$. Interactions types are abbreviated with HBA for hydrogen bond acceptor and HY for hydrophobic contact.

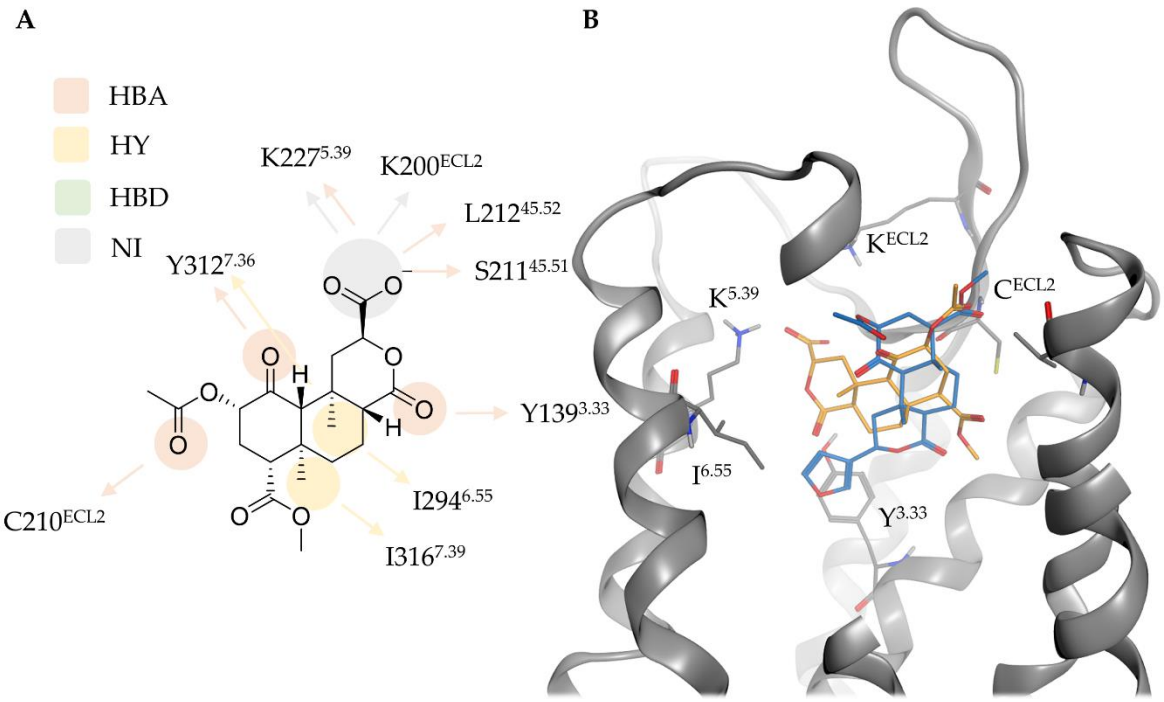

Figure S13. Protein-ligand interactions (A) and binding mode (B) of **13** (orange) at the KOR in comparison to SalA (blue). $Y^{3.33}$ denotes to $Y139^{3.33}$, C^{ECL2} to $C210^{ECL2}$, and $I^{6.55}$ to $I294^{6.55}$. Interactions types are abbreviated with HBA for hydrogen bond acceptor, HY for hydrophobic contact, HBD for hydrogen bond donor, and NI for negative charged interaction.

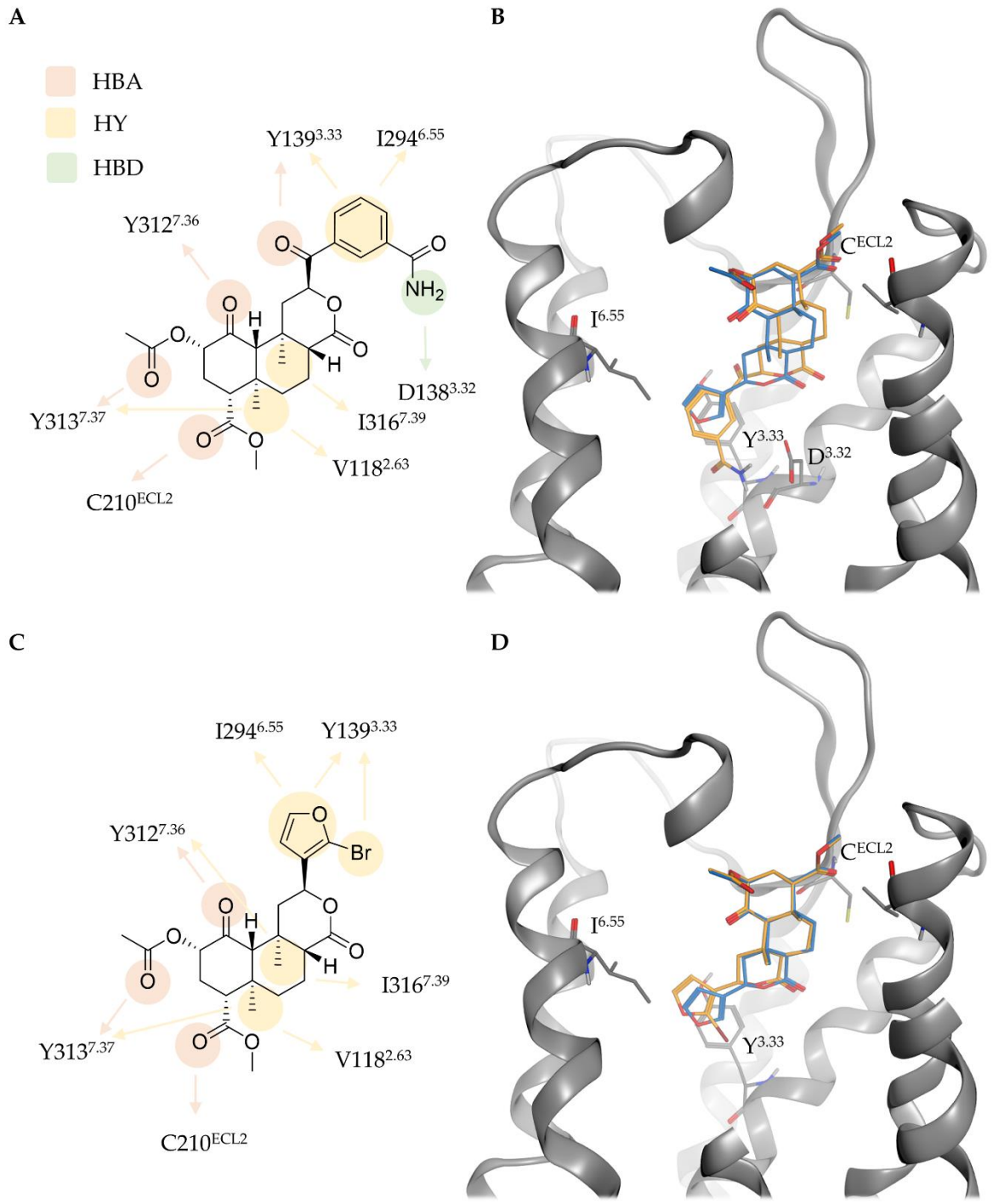

Figure S14. Protein-ligand interactions and binding mode of **14** (A, B, orange) and **15** (C, D, orange) at the KOR in comparison to SalA (blue). $Y^{3.33}$ denotes to $Y139^{3.33}$, C^{ECL2} to $C210^{ECL2}$, and $I^{6.55}$ to $I294^{6.55}$. Interactions types are abbreviated with HBA for hydrogen bond acceptor and HY for hydrophobic contact.

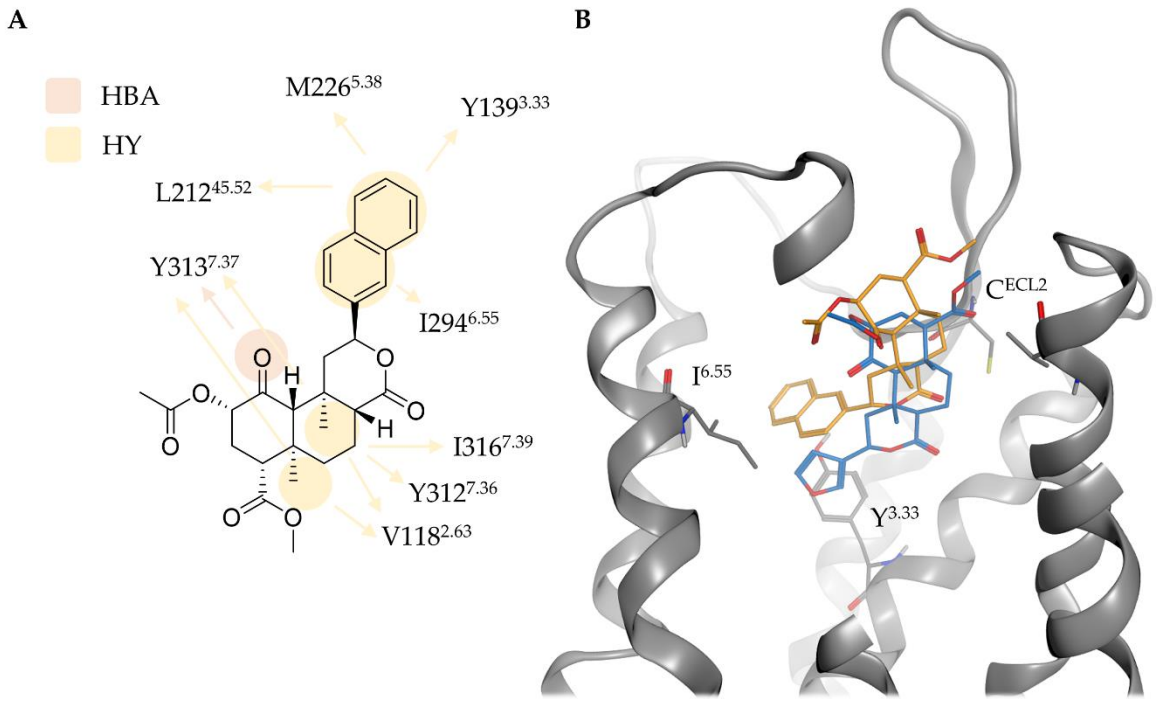

Figure S15. Protein-ligand interactions (A) and binding mode (B) of **16** (orange) at the KOR in comparison to SalA (blue). Y$^{3.33}$ denotes to Y139$^{3.33}$, C^{ECL2} to C210^{ECL2}, and I$^{6.55}$ to I294$^{6.55}$. Interactions types are abbreviated with HBA for hydrogen bond acceptor and HY for hydrophobic contact.

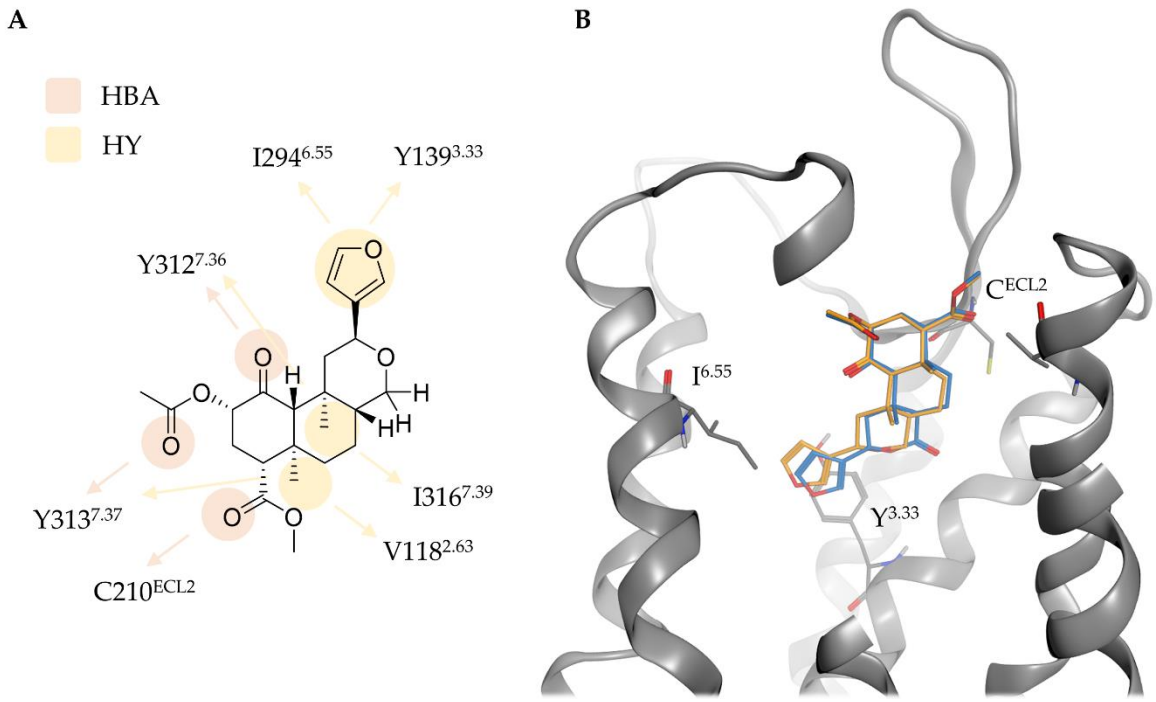

Figure S16. Protein-ligand interactions (A) and binding mode (B) of **17** (orange) at the KOR in comparison to SalA (blue). $Y^{3.33}$ denotes to $Y139^{3.33}$, C^{ECL2} to $C210^{ECL2}$, and $I^{6.55}$ to $I294^{6.55}$. Interactions types are abbreviated with HBA for hydrogen bond acceptor and HY for hydrophobic contact.

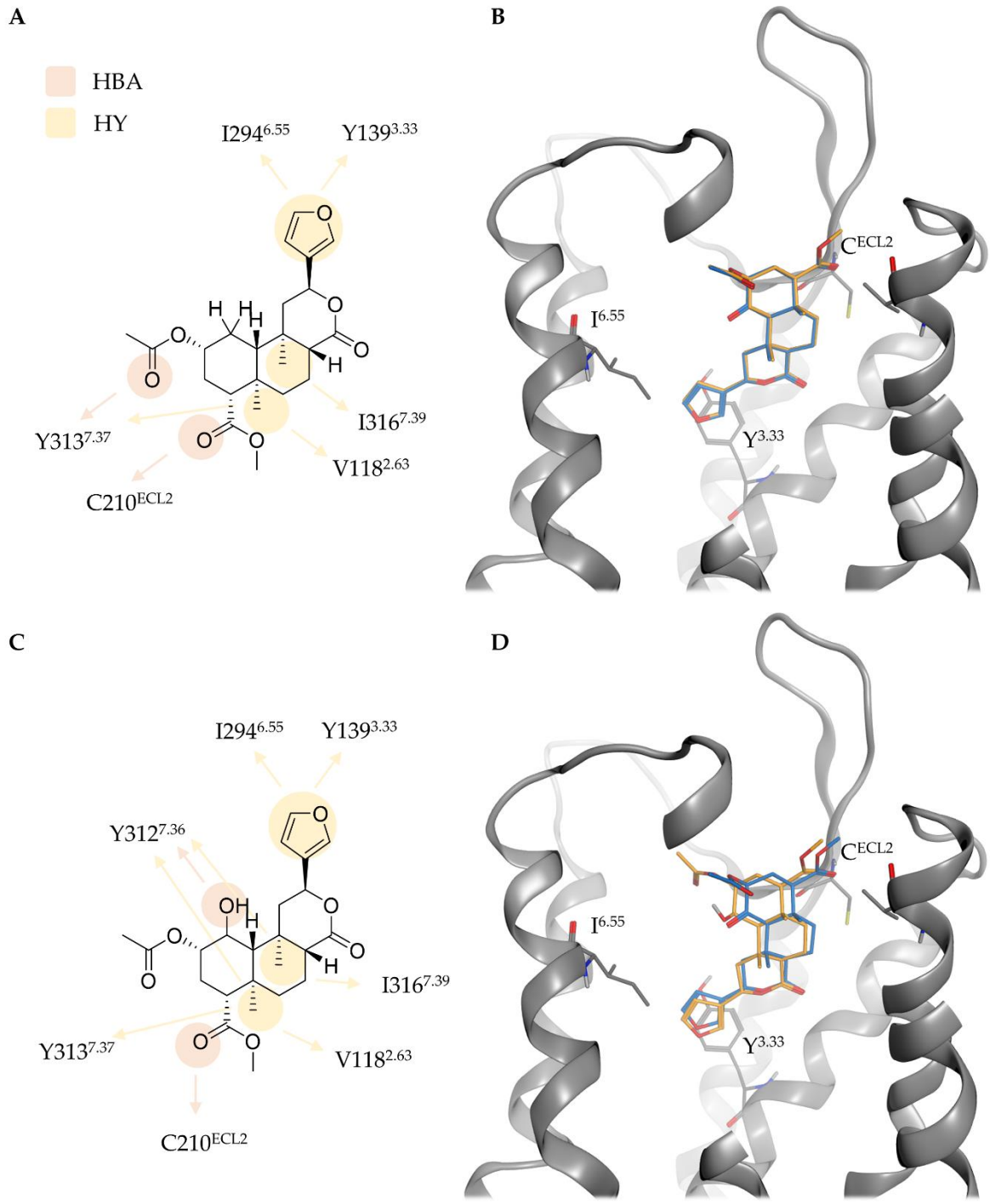

Figure S17. Protein-ligand interactions and binding mode of **18** (A, B, orange) and **19** (C, D, orange) at the KOR in comparison to SalA (blue $Y^{3.33}$ denotes to $Y139^{3.33}$, C^{ECL2} to $C210^{ECL2}$, and $I^{6.55}$ to $I294^{6.55}$. Interactions types are abbreviated with HBA for hydrogen bond acceptor and HY for hydrophobic contact.

References:

1. Gowers, R.J.; Alibay, I.; Swenson, D.W.H.; Henry, M.M. *Open Free Energy (openfe)*, version 0.21; 2022.
2. D E Shaw Research. *Desmond Molecular Dynamics System*, 2022-1; D E Shaw Research: New York, NY, USA, 2022.
3. Bowers, K.J.; Chow, D.E.; Xu, H.; Dror, R.O.; Eastwood, M.P.; Gregersen, B.A.; Klepeis, J.L.; Kolossvary, I.; Moraes, M.A.; Sacerdoti, F.D.; et al. Scalable algorithms for molecular dynamics simulations on commodity clusters. In Proceedings of the Proceedings of the ACM/IEEE Conference on Supercomputing (SC06), Tampa, FL, USA, 11-17 November 2006.
4. Rizzi A; Grinaway P.B.; Parton D.L.; Shirts M.R.; Wang K.; Eastman P.; Friedrichs M.; Pande V.S.; Branson K.; Mobley D.L.; et al. YANK: A GPU-accelerated platform for alchemical free energy calculations. http://getyank.org/latest/, accessed on December 1, 2022.
5. Che, T.; Majumdar, S.; Zaidi, S.A.; Ondachi, P.; McCorvy, J.D.; Wang, S.; Mosier, P.D.; Uprety, R.; Vardy, E.; Krumm, B.E.; et al. Structure of the nanobody-stabilized active state of the kappa opioid receptor. Cell **2018**, 172, 55-67.e15, doi:10.1016/j.cell.2017.12.011.